

## Synthesis of Flower-like Ag-ZnO Nanostructure and its Application in the Photodegradation of Methyl Orange

*Mansour Arab Chamjangali\* and Samira Boroumand*

*College of Chemistry, Shahrood University of Technology, Shahrood,  
PO Box 36155-316, Islamic Republic of Iran*

Materiais nanoestruturados do tipo Ag-ZnO foram sintetizados primeiro preparando um ZnO com morfologia de flor por um método de precipitação e então depositando partículas de Ag diretamente sobre sua superfície, utilizando um método simples de fotoredução. As estruturas foram caracterizadas por microscopia eletrônica de varredura (SEM) e de transmissão (TEM), difratometria de raios X (XRD) e espectrometria de absorção atômica (AAS). Os resultados mostraram que elas são compostas por nanopartículas de Ag metálica dispersas sobre a superfície de ZnO na forma de flor. O efeito fotocatalítico do Ag-ZnO na fotodegradação de alaranjado de metila (MO) sob radiação UV foi investigado em suspensão aquosa. Fatores que influenciam na reação de degradação e descolorização fotocatalítica do MO como pH, teor de Ag, tempo de fotodegradação, concentração do corante orgânico e presença de interferentes tais como  $Mg^{2+}$ ,  $Ca^{2+}$ ,  $NO_3^-$ ,  $Cl^-$  e  $SO_4^{2-}$  foram estudados. Resultados satisfatórios foram obtidos quando o método fotocatalítico proposto foi aplicado na degradação de MO em várias amostras de água residuais sintéticas.

Nanostructured Ag-ZnO materials were successfully synthesized by first producing a ZnO with flower-like morphology using a simple precipitation method, and then Ag nanoparticles were prepared directly on the surface by a facile photoreduction method. The materials were characterized by scanning and transmission electron microscopy (SEM and TEM), by X-ray diffractometry (XRD) and atomic absorption spectrometry (AAS). They were shown to be composed of metallic Ag particles dispersed on the surface of flower-like ZnO structures. Photocatalytic effect of Ag-ZnO on the photodegradation of methyl orange (MO) under UV irradiation was investigated in aqueous suspension. The effect of pH, Ag content, photodeposition time, concentration of the organic dye and presence of  $Mg^{2+}$ ,  $Ca^{2+}$ ,  $NO_3^-$ ,  $Cl^-$  and  $SO_4^{2-}$  on the photocatalytic degradation and decolorization reaction of MO was studied. The photocatalytic method was applied for the degradation of MO in several synthetic wastewater samples with satisfactory results.

**Keywords:** photoreduction, photocatalytic, Ag-ZnO, photodegradation, methyl orange

### Introduction

Wastewaters resulting from human activities can contain many organic and inorganic substances and are one of the main sources of environmental pollution due to the rapid development of industries. Anthraquinone, arylmethane, indigoid and azo dyes, used in large-scale particularly in textile industries, can produce toxic substances through oxidation, hydrolysis or other chemical reactions occurring in the waste water phase.<sup>1</sup> For this reason, the development of procedures to control or destroy this type of pollution is of great interest and a challenge.

Up to the present time, different methods have been developed for removing colored pollutants from wastewaters. The most common methods are coagulation/flocculation and removal by activated carbon,<sup>2</sup> that generate huge amounts of sludge and waste, which should be disposed of. A new and effective approach for removal and degradation of dyes are the advanced oxidation processes (AOPs). Among the different AOPs, the photoassisted catalytic decomposition of organic pollutants, employing semiconductors as photocatalysts, are promising.  $TiO_2$  and ZnO are the most favorable photocatalytic materials for the photoassisted catalytic decomposition of organic contaminants. Both materials exhibit very similar band gaps (ZnO, 3.37 eV;  $TiO_2$ , 3.2 eV) and conduction band edge positions.<sup>3</sup> Although  $TiO_2$  is widely employed as photocatalyst, ZnO is a low-cost

\*e-mail: arabe51@yahoo.com

alternative.<sup>4</sup> Higher photocatalytic efficiencies of ZnO have also been reported, especially for degradation of organics in aqueous solution.<sup>5-7</sup> Recent reports have shown that the morphology and dimensionality of ZnO have a great effect on its photocatalytic activity.<sup>8,9</sup> Therefore, synthesis and application of 3D ZnO nanostructures with different morphologies are now important to confirm their potential. Recently, efforts have been focused on the preparation of ZnO nanostructures with various morphologies including the tower-like,<sup>10</sup> dumbbell-like,<sup>11</sup> nut-like<sup>12</sup> and flower-like.<sup>13,14</sup> Among them, flower-like ZnO showed a strong morphology-induced enhancement of photocatalytic performance.<sup>15</sup> Additionally, the modification of semiconductor surface by noble metal deposition can be used to improve their photocatalytic activity.<sup>16-22</sup> The photogenerated electrons in the conduction band can be transferred to the noble metal nanoparticles (NPs) due to the Schottky barrier formed at the metal-semiconductor interface,<sup>23,24</sup> whereas holes can remain on the semiconductor surface. Thus, the noble metals can act as an electron sink, facilitating the charge separation and improving the photocatalytic efficiency. In fact, Ag NPs have been widely used for modification of the ZnO surface to enhance the activity for photocatalytic degradation or decolorization of organic dyes.<sup>25-35</sup> Although there are reports about the synthesis of Ag-ZnO composite, there is still no facile method to synthesize novel and uniform Ag-ZnO nanostructures. To the best of our knowledge, the synthesis of flower-like Ag-ZnO nanostructures via a coupled solution route/photoreduction process, and a detailed investigation on their activity towards the photodegradation of methyl orange (MO) have not been reported in the literature. Thus, the detailed comparative studies carried out, under the optimal conditions for photodegradation of the MO dye in aqueous solution, in the presence of the flower-like ZnO and Ag-ZnO nanostructures are reported here.

## Experimental

### Chemicals

Chemicals including silver nitrate and zinc acetate dehydrate were supplied from Aldrich, and sodium hydroxide, MO and poly(vinyl pyrrolidone) (PVP) were purchased from Merck. The other chemicals were of analytical reagent grade, and were used as received without further purification. Water distilled three times was used throughout.

### Instruments

Transmission electron microscopy (TEM) images were obtained using a Philips CM120 TEM. X-ray

diffraction (XRD) patterns were obtained using a Bruker AXS (Model B8-Advance) diffractometer with Cu K $\alpha$  radiation ( $\lambda$  at 0.15418 nm). Scanning electron microscopy (SEM) analysis was conducted using a Hitachi S-4160 electron microscope. A Shimadzu model AA-670 flame atomic absorption spectrometer with an air-acetylene flame, equipped with a silver hollow cathode lamp was used for quantification of silver content under the conditions recommended by the manufacturer. The UV-Vis spectra were recorded in a double beam Rayleigh UV-2601 UV-Vis spectrophotometer using a pair of 1.0 cm quartz cells. The pH measurements and adjustments were carried out using a Metrohm 744 pH-meter equipped with a combined glass electrode. A Hettich centrifuge model Rotine 380 was used for separation of precipitates from solution. A high pressure Philips mercury lamp (400 W) was used as UV irradiation source.

### Preparation of ZnO with flower-like morphology

The flower-like ZnO structure was synthesized according to the method reported for synthesis of Ag-ZnO by Krishna *et al.*<sup>36</sup> with some modifications. Typically, a total of 25 mL of water was heated in a beaker to reach a constant temperature of 60 °C. Then, 250 mL of aqueous PVP solution (12.5 mg mL<sup>-1</sup>) and subsequently 25 mL of zinc acetate (0.10 mol L<sup>-1</sup>) were added, at 60 °C. The solution was homogenized by constant stirring for about 1 min, and then 25.0 mL of NaOH (0.50 mol L<sup>-1</sup>) were added, and stirred at 60 °C for 1 h. The ZnO precipitate was then collected by centrifugation, washed with deionized water and ethanol several times, dried at 80 °C for 4 h, and used for subsequent preparation of the flower-like Ag-ZnO materials.

### Synthesis of Ag-ZnO

The Ag nanoparticles were prepared directly on the flower-like ZnO surface by photoreduction of Ag<sup>+</sup> ions to Ag NPs by UV irradiation. In brief, 0.20 g of flower-like ZnO was transferred into a 250 mL beaker, dispersed in 30 mL of water and irradiated with a 400 W high-pressure mercury lamp, placed 12 cm above the solution surface for 10 min, to remove the impurities present on the surface. Then, AgNO<sub>3</sub> (0.30-1.2 mmol) was added, the suspension diluted to about 100 mL, stirred at 500 rpm in the dark for 15 min to achieve desorption/adsorption equilibrium of silver ions at room temperature, and purged with pure N<sub>2</sub> gas for 5 min. Then, it was irradiated with a 400 W UV lamp for 40 min, while purging with nitrogen. The precipitate was separated by centrifugation, washed with distilled water and ethanol repeatedly to remove the residual Ag<sup>+</sup> ions, and

dried at 80 °C for 4 h. The amount of Ag present in each sample was controlled by the amount of AgNO<sub>3</sub> and the UV irradiation time. The amount of Ag<sup>+</sup> loaded on the surface of ZnO was obtained using atomic absorption spectrometry (AAS), and the weight percentages (wt.%) of Ag were calculated for all samples. The experimental conditions for the synthesis of Ag-ZnO samples and respective percentage in weight of Ag nanoparticles are summarized in Table 1.

**Table 1.** Characterization and reaction conditions for samples S1-S9

Sample	AgNO <sub>3</sub> / mmol	Irradiation time / min	Ag / wt. %
S1	0.30	40	16.7
S2	0.45	40	21.6
S3	0.60	40	23.2
S4	0.90	40	25.1
S5	1.2	40	26.0
S6	0.90	10	6.3
S7	0.90	60	28.0
S8	0.90	80	31.0
S9	0.90	100	35.0

#### Procedure for photocatalytic degradation/decolorization studies

Many photocatalytic experiments were carried out using a homemade photoreactor (120 cm × 100 cm × 100 cm), and the 400 W mercury lamp for UV irradiation. The distance between the solution surface and the light source was about 12 cm. In a typical experiment, 100 mL of aqueous MO with an initial concentration of 10 mg L<sup>-1</sup> (pH 7.0) were placed in a beaker, the photocatalyst (300 mg L<sup>-1</sup>) added and the suspension stirred for 40 min in the dark, at room temperature, to ensure the establishment of the adsorption/desorption equilibrium. Then, the UV lamp was turned on while the suspension was magnetically stirred. At fixed intervals of time, 2 mL of sample were withdrawn, centrifuged, and the supernatant transferred into a spectrophotometer cell for measurement of the absorbance of MO at 464 and 272 nm.

## Results and discussion

### Characterization of the photocatalyst

#### XRD spectra

The XRD patterns for the flower-like morphology of ZnO and Ag-ZnO nanostructures with different Ag contents are shown in Figure 1. All peaks (Figure 1a) are consistent

with the hexagonal wurtzite structure of ZnO with the estimated lattice constants  $a = 3.2498 \text{ \AA}$  and  $c = 5.2066 \text{ \AA}$ . The main diffraction peaks for the Ag-ZnO samples (Figures 1b-1f) can be readily indexed to two groups. The first group of peaks (100), (002), (101), (102), (110) and (103) matches well with the ZnO standard wurtzite structure like the bare ZnO (Figure 1a). The second group of peaks (111), (200) and (220) is in good agreement with the face-centered cubic (fcc) metallic Ag (JCPDS 04-0783) with lattice constant  $a = 4.0862 \text{ \AA}$ . This confirms that silver atoms are not incorporated into the ZnO lattice but are loaded onto the ZnO surface.

Some further studies were carried out to investigate the effect of the initial amount of AgNO<sub>3</sub> and UV irradiation time on the quantity of loaded Ag, lattice structures of ZnO or Ag, and size of Ag NPs. In this study, the Ag-ZnO samples (S2, S4, S5, S6 and S8) were prepared under the conditions given in Table 1, and their XRD spectra were recorded (Figures 1b-1f). The diffraction peaks agree with metallic Ag and ZnO structures and no impurity phases were detected even for high initial relative amounts of AgNO<sub>3</sub> or long UV irradiation time. The intensity ratio of the (111) plane of metallic Ag and the (101) plane of ZnO diffraction peaks, ( $\frac{I_{111}}{I_{101}}$ ), was calculated for each sample. According to the data given in Table 2, it is clear that by increasing the amount of AgNO<sub>3</sub> or irradiation time during the photodeposition of Ag, the ( $\frac{I_{111}}{I_{101}}$ ) ratio increases. This points out the positive correlation between the amount of AgNO<sub>3</sub> or irradiation time and the amount of Ag loaded, which is in accord with the AAS results (Table 1). The size of ZnO and Ag NPs calculated by the Debye-Scherrer equation (Table 2) showed that there is no significant effect of the initial concentration of AgNO<sub>3</sub> and irradiation time on the size of the Ag and ZnO NPs.

### SEM and TEM images

The morphology, size and microstructure of ZnO and Ag-ZnO samples were investigated in detail by SEM (Figure 2). They consisted of 300 nm wide and 400 nm long flower-like microstructures with average size of ca. 1-2 μm composed of about 4-5 nanoleaves (enlarged images). By comparing the morphologies of ZnO (Figure 2a) and Ag-ZnO (Figure 2b), it is clear that the ZnO morphology has not been changed upon modification with Ag NPs. Figure 3 shows the TEM image of a typical Ag-ZnO flower-like structure, confirming the results obtained by SEM.

### Photocatalytic activity of Ag-ZnO

Figure 4 shows the absorption spectra of 100 mL MO (10 mg L<sup>-1</sup>) as a function of UV irradiation time in the

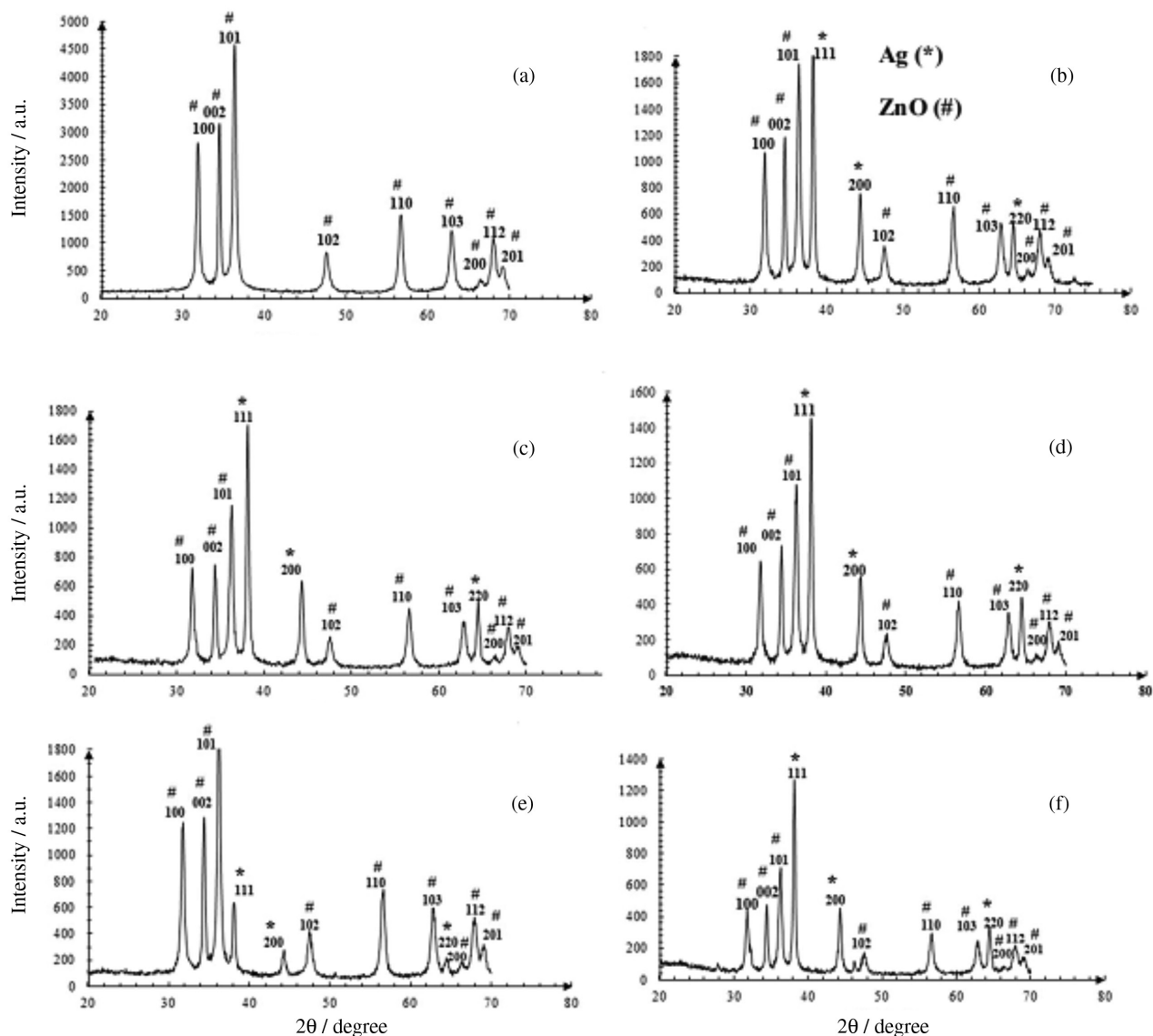


**Figure 1.** XRD patterns for the ZnO and Ag-ZnO flower-like samples synthesized under the reaction conditions summarized in Table 1: (a) ZnO, (b) S<sub>2</sub>, (c) S<sub>4</sub>, (d) S<sub>5</sub>, (e) S<sub>6</sub> and (f) S<sub>8</sub>. Ag (\*) and ZnO (#).

**Table 2.** The intensity ratios of XRD peaks (the (111) plane of metallic Ag to the (101) plane of ZnO) and size of nanoparticles for flower-like ZnO and Ag-ZnO samples

Sample	$\frac{I_{111}}{I_{101}}$	Size of nanoparticle / nm	
		ZnO	Ag
ZnO	–	18.0	–
S <sub>2</sub>	1.23	19.0	24.0
S <sub>4</sub>	1.35	17.0	21.0
S <sub>5</sub>	1.36	20.0	23.0
S <sub>6</sub>	0.322	18.0	21.0
S <sub>8</sub>	1.78	17.0	24.0

presence of 300 mg L<sup>-1</sup> Ag-ZnO (sample S<sub>4</sub>) at pH 7.0 and room temperature. The changes in the absorbance at

464 nm are due to breaking of the azo bonds, leading to the bleaching of MO (decolorization). On the other hand, changes in the absorbance at 272 nm are correlated with the concentration of organic residuals in solution, and thus to the mineralization (degradation) of the organic dye. No significant change was observed in the concentration of MO after 30 min, in the dark (no UV light irradiation), indicating that the adsorption process reached the equilibrium condition. Thus, in all experiments, the suspensions containing MO and photocatalysts were continuously stirred for 40 min in the dark in order to ensure the adsorption/desorption equilibrium. The results obtained for the photocatalytic degradation/decolorization of MO using the Ag-ZnO and ZnO nanoflowers as photocatalyst are presented in Figure 5.

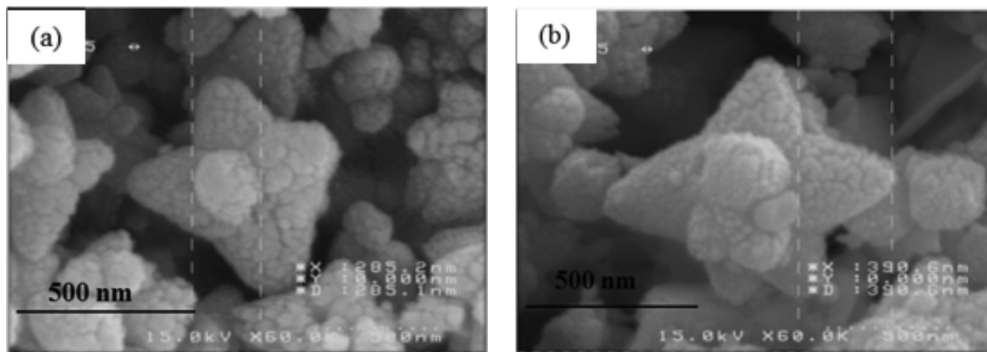


Figure 2. SEM images of (a) ZnO and (b) Ag-ZnO (sample  $S_4$ ).

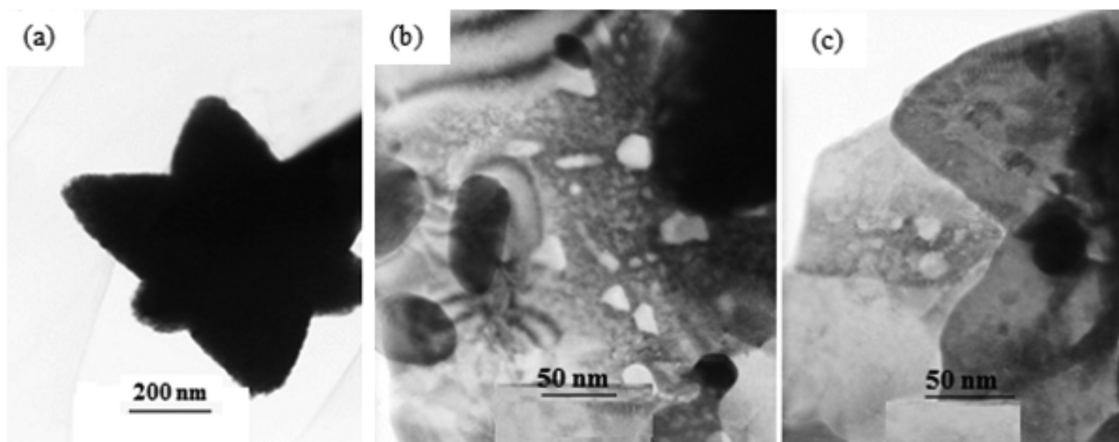


Figure 3. TEM images of Ag-ZnO (sample  $S_4$ ): (a) is in a lower magnification than (b) and (c).

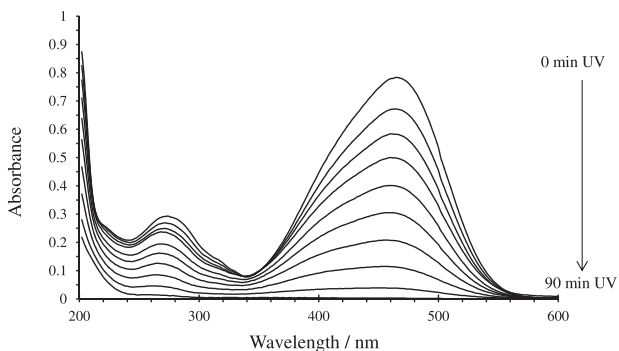


Figure 4. UV-Vis absorbance spectra for MO solution in the presence of Ag-ZnO as a function of UV-light exposure time. Conditions:  $10.0 \text{ mg L}^{-1}$  MO; Ag-ZnO (sample  $S_4$ ),  $300 \text{ mg L}^{-1}$  and pH 7.0 at room temperature.

The photodegradation of MO under UV irradiation in the absence of photocatalyst is not significant and could be ignored. As shown in Figure 5, Ag-ZnO displayed a higher photocatalytic activity than pure ZnO. The dye was completely degraded or decolorized in 90 min in the presence of the Ag-ZnO flower-like material, but only 47.2% of degradation and 65.7% of decolorization was observed using bare ZnO as catalyst. Those results confirmed the more effective electron-hole separation in the flower-like Ag-ZnO structure, which can be assigned

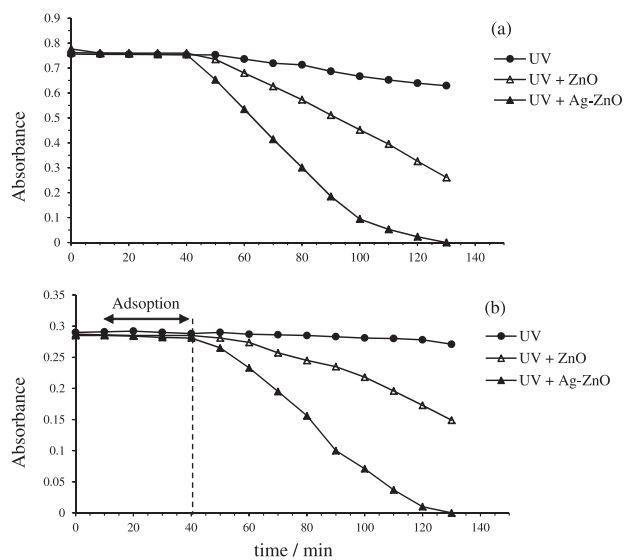


Figure 5. Decolorization (a) and degradation (b) rates of MO. Conditions:  $10.0 \text{ mg L}^{-1}$  MO; Ag-ZnO (sample  $S_4$ ),  $300 \text{ mg L}^{-1}$  and pH 7.0 at room temperature.

to the fact that Ag NPs act as electron sinks, enhancing the interfacial charge transfer kinetics between the metal and semi-conductor, and thus enhancing the photocatalytic activity of Ag-ZnO.<sup>37</sup>

### Optimization of the photocatalytic conditions

In the optimization procedure, the efficiency (E) percentages the degradation and decolorization processes were used to monitor the photocatalytic activity, which was calculated as follows:

$$E (\%) = \frac{C_0 - C_t}{C_0} 100, \quad (1)$$

where  $C_0$  is the concentration of MO in adsorption/desorption equilibrium in the dark ( $t = 0$ ), and  $C_t$  is the concentration of MO remaining at reaction time  $t$  (min). The concentration of MO dye in solution was determined spectrophotometrically in triplicate, at 464 (decolorization) and 272 nm (degradation), using suitable calibration curves.

### The pH effect

The solution pH is an important operational parameter, playing a significant role in the photocatalytic degradation of various pollutants. The pH effect on the photodegradation of MO was studied in the 3.0-10.0 range, at room temperature. Suspensions with  $\text{pH} < 3.0$  were not considered due to the dissolution of ZnO. The solution pH was adjusted with nitric acid or sodium hydroxide before irradiation, and it was not controlled during the course of the reaction. Figure 6 shows that the degradation and decolorization efficiencies increase as a function of pH up to 7.0, and then decrease at higher pH values. Thus, pH 7.0 was selected as the optimal condition for all photocatalytic experiments. The overall degradation rate at the semiconductor/liquid interface is influenced to some extent by the surface properties. The metal oxide surface charge is a function of solution pH. For ZnO, the pH of the point of zero charge ( $\text{pH}_{\text{pzc}}$ ) is found in the 6.9 to 9.8 range.<sup>38</sup> So, the ZnO surface is presumably positively charged in acidic solutions ( $\text{pH} < \text{pH}_{\text{pzc}}$ ) and negatively charged in alkaline solutions. On the other hand,

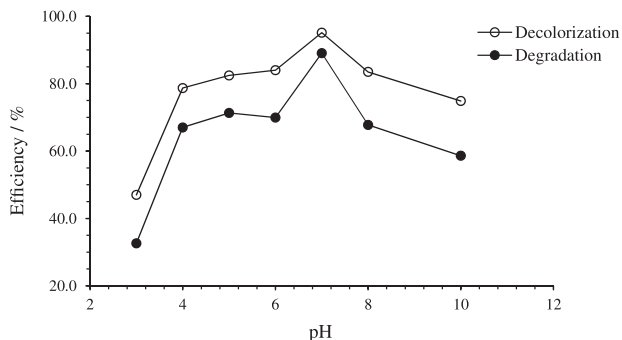


**Figure 6.** The pH effect on the degradation and decolorization of MO. Conditions: 10.0 mg L<sup>-1</sup> MO; Ag-ZnO (sample S<sub>2</sub>), 200 mg L<sup>-1</sup>; irradiation time of 70 min at room temperature.

the proportion of the negatively charged MO ( $\text{pK}_a = 4$ ) species increases with the increase in the solution pH. Accordingly, the adsorption of MO dye onto ZnO and the degradation efficiency of MO should increase as a function of pH, due to electrostatic attraction. Moreover, at higher pH values, the OH<sup>-</sup> ions should compete with the dye for the adsorption sites, inhibiting the dye adsorption.

### Effect of AgNO<sub>3</sub> concentration in the deposition solution

It is clear that the weight percentage of Ag in Ag-ZnO increases with the increase in the initial concentration of AgNO<sub>3</sub> and this parameter has considerable effect on the photocatalytic activity of Ag-ZnO. Therefore, the relation between the photocatalytic activity of Ag-ZnO and the initial concentration of the AgNO<sub>3</sub> solution used for Ag deposition was studied. For this purpose, the photocatalytic activities of 200 mg L<sup>-1</sup> of different Ag-ZnO catalysts (samples S1 to S5, in Table 1) for the degradation/decolorization of 100 mL of MO (10.0 mg L<sup>-1</sup>) were measured at room temperature. As shown in Figure 7, the photocatalytic activity increased with the Ag content up to 25.1 wt.%. However, the photocatalytic activity of Ag-ZnO decreases at larger Ag contents probably because the metal deposits reversely act as recombination centers. The over accumulations of electrons on metal deposits could attract the photogenerated holes to the metal sites, and thus facilitating the recombination of charge carriers.<sup>37,39</sup> In addition, higher surface loadings may reduce the light absorption and pollutant adsorption by the semiconductor.<sup>40</sup> Thus, the optimal Ag content is approximately 25.1 wt.%, which could be obtained by using a deposition solution with  $9.0 \times 10^{-3}$  mol L<sup>-1</sup> of AgNO<sub>3</sub> and 40 min photodeposition time.

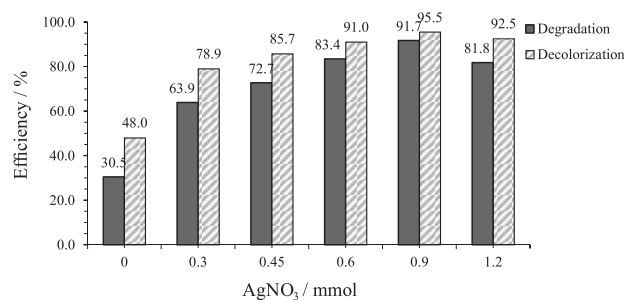


**Figure 7.** Decolorization and degradation of MO by Ag-ZnO with increasing Ag content under UV irradiation time of 70 min. Conditions: 10.0 mg L<sup>-1</sup> MO; ZnO and/or Ag-ZnO (samples S<sub>1</sub>-S<sub>5</sub>), 200 mg L<sup>-1</sup> and pH 7.0 at room temperature.

### Effect of photodeposition time on the photocatalytic activity

The photocatalytic activity of Ag-ZnO is also dependent on the photodeposition time. This dependence was

studied by measuring the photocatalytic activity of the Ag-ZnO catalyst prepared under different photodeposition times (samples S4 and S6 to S9, in Table 1). The results obtained for the degradation/decolorization of 100 mL of MO (10.0 mg L<sup>-1</sup>) in the presence of 200 mg L<sup>-1</sup> Ag-ZnO (Figure 8) at room temperature show that for the same AgNO<sub>3</sub> deposition solution, the photocatalyst activity increased with the photodeposition time up to 40 min and then declines, as expected for the lower light absorption and increased electron-hole recombination centers as a function of the relative amount of loaded Ag (Table 1).

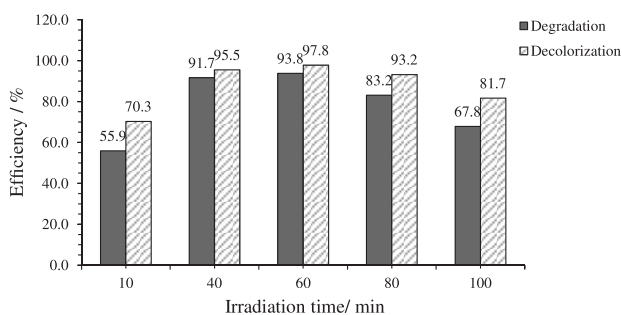


**Figure 8.** Decolorization and degradation of MO under UV irradiation time of 70 min by Ag-ZnO under different UV irradiation time during the synthesis process. Conditions: 10.0 mg L<sup>-1</sup> MO; Ag-ZnO (S<sub>4</sub> and S<sub>6</sub>-S<sub>9</sub>), 200 mg L<sup>-1</sup> and pH 7.0 at room temperature.

#### Effect of Ag-ZnO amount

The photocatalytic degradation and decolorization of MO was also investigated at a fixed concentration of MO (10.0 mg L<sup>-1</sup>) in pH 7.0 aqueous solution in the presence of increasing amounts of Ag-ZnO (with 25.1% Ag content), at room temperature. The efficiency percentage increased as a function of the amount of catalyst up to about 300 mg L<sup>-1</sup>, and then marginally decreased with further increase in the amount of catalyst. It is well-known that the increase in the amount of catalyst increases the number of active sites on the photocatalyst surface, which in turn increases the number of hydroxyl and superoxide radicals. On the other hand, the increase in the catalyst concentration beyond the optimum condition may result in the agglomeration of catalyst particles. Hence part of the catalyst surface becomes unavailable for photon absorption, thus the capture of the light by the suspension decreases, decreasing the photocatalytic activity.<sup>41</sup> Therefore, 300 mg L<sup>-1</sup> of catalyst was chosen as the optimal condition that was used in the subsequent studies.

#### Initial dye concentration effect

From the application point of view, the study of the dependence of the photocatalytic performance on

the dye concentration is very important. Therefore, the effect of initial dye concentration on the photocatalytic degradation and decolorization was investigated in the 5.0-20 mg L<sup>-1</sup> range, in the presence of 300 mg L<sup>-1</sup> catalyst (sample S<sub>4</sub>), at pH 7.0 and room temperature. As shown in Figure 9, the efficiency percentages for both degradation and decolorization decreased as the initial MO concentration increased because a larger fraction of photons is absorbed directly by the dye molecules before they can reach the catalyst surface. Additionally, more dye molecules are adsorbed on the surface of Ag-ZnO decreasing the concentration of active sites for adsorption of hydroxyl ions and generation of hydroxyl radicals.<sup>42</sup>

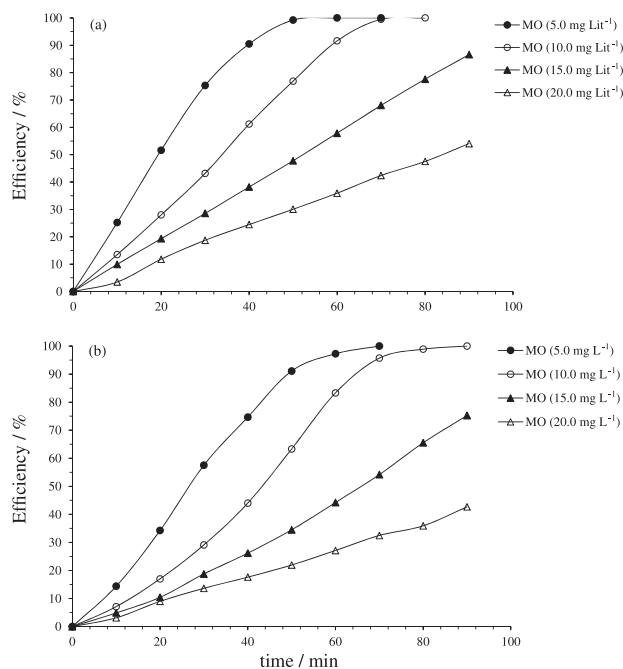


**Figure 9.** Effect of the initial dye concentration on the decolorization efficiency (a) and degradation efficiency (b) of MO. Conditions: Ag-ZnO (S<sub>4</sub>), 300 mg L<sup>-1</sup> and pH 7.0 at room temperature.

#### Effect of dissolved oxygen

The effect of dissolved O<sub>2</sub> on the photocatalytic degradation/decolorization of MO was studied by taking 10.0 mg L<sup>-1</sup> MO solution and 300 mg L<sup>-1</sup> catalyst (sample S<sub>4</sub>) at pH 7, at room temperature. The dissolved oxygen was removed from the solution by purging the photocatalyst and MO suspension with high purity N<sub>2</sub> in the dark for 30 min. The decolorization and degradation efficiencies in air and 70 min UV irradiation were 99.5 and 95.7%, whereas analogous experiments in N<sub>2</sub> atmosphere resulted in 85.6 and 51.7% of decolorization and degradation, respectively. These results confirmed that the oxygen content is an important factor for the photocatalytic

process because superoxide radicals may be formed when it reacts with the electrons generated in the process. These radicals can further react with water molecules, eventually forming hydroxyl radicals.<sup>28</sup>

#### Kinetic study

The investigation of kinetics of dye decolorization is often confusing because the process is complex. It is often believed that degradation and decolorization mechanisms depend on the surface coverage of the catalyst ( $\theta$ ). If the dye concentration is very low ( $\theta \ll 1$ ), the rate equation is rendered into the first-order kinetics. On the other hand, at relatively higher dye concentration ( $\theta$  ca. 1), the mechanism follows the zero-order kinetics.<sup>43</sup> In order to investigate the reaction kinetics the MO concentration was monitored as a function of time and initial MO concentration in the 10.0-20.0 mg L<sup>-1</sup> range. The same amount of catalyst (300 mg L<sup>-1</sup>) was used and the data compared with first- and zero-order kinetics. A plot of  $[\text{MO}]_t$  vs. irradiation time (t) should give an exponential curve if the reaction mechanism follows first-order kinetics, and if the mechanism is zero-order kinetics, the plot should be a straight line. In our case, straight lines ( $R^2$ ; 0.9892-0.9999) were found when  $[\text{MO}]_t$  was plotted against irradiation time, indicating that the concentration was sufficient to form a monolayer coverage ( $\theta$  ca. 1) on the Ag-ZnO surface. From the slope of the zero-order kinetics curves, the apparent rate constants of  $(3.5 \pm 0.2) \times 10^{-7}$  and  $(4.5 \pm 0.2) \times 10^{-7}$  mol L<sup>-1</sup> s<sup>-1</sup> were calculated for degradation and decolorization of MO, respectively.

#### Reuse of the Ag-ZnO catalyst

Ag-ZnO recycling can be foreseen as a good practice for sustainable wastewater treatment. Consequently, it is necessary to demonstrate whether, after a photocatalytic treatment, the catalyst can be reused. The Ag-ZnO catalyst was recycled and reused five consecutive times for MO degradation using 300 mg L<sup>-1</sup> of catalyst. After each experiment, the catalyst was separated by centrifugation, thoroughly washed with distilled water and ethanol, and reused for the next photodegradation experiment. The efficiency was evaluated for each reuse cycle after 70 min and the results summarized in Table 3. The Ag-ZnO photocatalyst (sample S<sub>4</sub>) exhibited nearly constant photostability up to three recycling processes, but the efficiency markedly decreased for the fourth and fifth cycles. However, the rate of degradation is still significant after five times of Ag-ZnO reuse. Agglomeration and sedimentation of the dye around Ag-ZnO particles after

each photocatalytic degradation cycle is a possible cause of the observed decrease of efficiency, because each time that the photocatalyst is reused, new parts of the catalyst surface become unavailable for dye adsorption and thus for photon absorption, reducing the efficiency of the catalytic reaction.

**Table 3.** Results obtained for reusing of Ag-ZnO (sample S<sub>4</sub>) after cyclic regeneration in the decolorization and degradation of 10.0 mg L<sup>-1</sup> of MO at pH 7.0 and room temperature

No. of cycles	Efficiency / %	
	Decolorization	Degradation
1	99.5	95.7
2	100.0	98.3
3	100.0	98.3
4	95.4	86.8
5	76.6	64.4

#### Interference study

Since different constituents can be present in wastewater, the basic understanding of the effect of foreign species on the performance of photocatalytic systems is important to ensure operational stability of a catalyst in the photocatalytic water purification process. Therefore, the influence of most common co-existing species on the degradation/decolorization of a MO solution (10.0 mg L<sup>-1</sup>) was investigated under the optimum conditions. The degradation/decolorization efficiencies of aqueous solutions containing 10.0 mg L<sup>-1</sup> MO and increasing amounts of possible interfering ions were measured under 90 min UV irradiation. The tolerance limit was defined as the concentration giving a change of 3S (S is the standard deviation of five replicates of degradation/decolorization efficiency measurements). The results shown in Table 4 indicated that common ions (even at high concentrations) do not have a significant interference effect on the photocatalytic activity of the Ag-ZnO catalyst

**Table 4.** Interference study results for the decolorization and degradation of 10.0 mg L<sup>-1</sup> MO in the presence of 300 mg L<sup>-1</sup> of Ag-ZnO (sample S<sub>4</sub>), at pH 7.0 and room temperature

Species	Tolerable concentration / (mg L <sup>-1</sup> )	
	Decolorization	Degradation
SO <sub>4</sub> <sup>2-</sup> , NO <sub>3</sub> <sup>-</sup>	1000 <sup>a</sup>	1000 <sup>a</sup>
Ca <sup>2+</sup>	500	100
Mg <sup>2+</sup>	400	400
Cl <sup>-</sup>	50	50

<sup>a</sup>Maximum concentration tested.

for the degradation of wastewater samples. The Ag-ZnO catalyst also showed satisfactory catalytic efficiency (93.5% efficiency after 90 min) for photodegradation of MO in untreated tap water spiked with MO at optimum conditions (Figure 10), confirming the previous results.

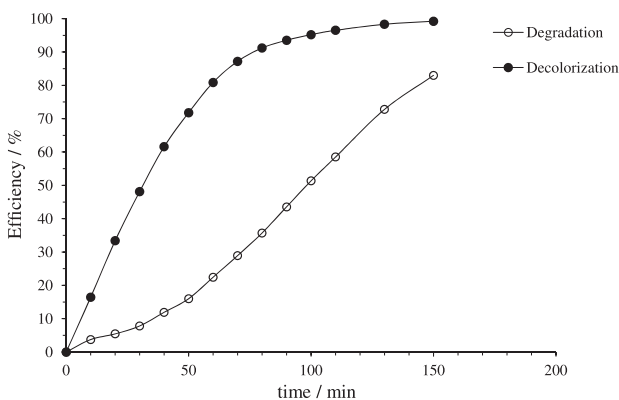


**Figure 10.** Photocatalytic decolorization and degradation efficiency of  $10.0 \text{ mg L}^{-1}$  MO in the synthetic waste water in the presence of  $300 \text{ mg L}^{-1}$  of Ag-ZnO (sample  $S_4$ ) at pH 7.0 and room temperature.

## Conclusion

MO was decomposed after 90 min UV irradiation in the presence of the nanoflower-like Ag-ZnO photocatalyst, showing an activity relatively higher than that of parent ZnO nanoflowers at neutral pH. The photocatalyst can be used three times without any change in its photocatalytic efficiency. Hence, based on its excellent performance, the Ag-ZnO nanoflower may be useful for the photocatalytic purification of water polluted by MO.

## Acknowledgement

The authors are thankful to the Shahrood University of Technology Research Council for supporting this work.

## Reference

- Robinson, T.; McMullan, G.; Marchant, R.; Nigam, P.; *Bioresour. Technol.* **2001**, *77*, 247.
- Melgoza, D.; Hernandez-Ramirez, A.; Peralta-Hernandez, J. M.; *Photochem. Photobiol. Sci.* **2009**, *8*, 596.
- Wang, N.; Sun, C.; Zhao, Y.; Zhou, S.; Chen, P.; Jiang, L.; *J. Mater. Chem* **2008**, *18*, 3909.
- Pawinrat, P.; Mekasuwandumrong, O.; Panpranot, J.; *Catal. Commun.* **2009**, *10*, 1380.
- Akyol, A.; Yatmaz, H. C.; Bayramoglu, M.; *Appl. Catal., B* **2004**, *54*, 19.
- Kavitha, R.; Meghani, S.; Jayaram, V.; *Mater. Sci. Eng., B* **2007**, *139*, 134.
- Daneshvar, N.; Salari, D.; Khataee, A. R.; *J. Photochem. Photobiol., A* **2004**, *162*, 317.
- Li, D.; Haneda, H.; Kawano, K.; Saito, N.; *J. Jpn. Soc. Powder Powder Metall.* **2001**, *48*, 1044.
- Li, D.; Haneda, H.; *Chemosphere* **2003**, *51*, 129.
- Wang, Z.; Qian, X.-F.; Yin, J.; Zhu, Z.-K.; *Langmuir* **2004**, *20*, 3441.
- Sun, J.-H.; Dong, S.-Y.; Wang, Y.-K.; Sun, S.-P.; *J. Hazard. Mater.* **2009**, *172*, 1520.
- Zheng, Y.; Yu, X.; Xu, X.; Jin, D.; Yue, L.; *Ultrason. Sonochem.* **2010**, *17*, 7.
- Liu, J.; Huang, X.; Li, Y.; Duan, J.; Ai, H.; *Mater. Chem. Phys.* **2006**, *98*, 523.
- Xie, J.; Li, Y.; Zhao, W.; Bian, L.; Wei, Y.; *Powder Technol.* **2011**, *207*, 140.
- Li, B.; Wang, Y.; *J. Phys. Chem. C* **2009**, *114*, 890.
- Subramanian, V.; Wolf, E. E.; Kamat, P. V.; *J. Phys. Chem. B* **2003**, *107*, 7479.
- Wu, J.-J.; Tseng, C.-H.; *Appl. Catal., B* **2006**, *66*, 51.
- Height, M. J.; Pratsinis, S. E.; Mekasuwandumrong, O.; Praserttham, P.; *Appl. Catal., B* **2006**, *63*, 305.
- Liqiang, J.; Dejun, W.; Baiqi, W.; Shudan, L.; Baifu, X.; Honggang, F.; Jiazhong, S.; *J. Mol. Catal. A: Chem.* **2006**, *244*, 193.
- Gouvêa, C. A. K.; Wypych, F.; Moraes, S. G.; Durán, N.; Peralta-Zamora, P.; *Chemosphere* **2000**, *40*, 427.
- Li, F. B.; Li, X. Z.; *Appl. Catal., A* **2002**, *228*, 15.
- Li, F. B.; Li, X. Z.; *Chemosphere* **2002**, *48*, 1103.
- Linsebigler, A. L.; Lu, G.; Yates, J. T.; *Chem. Rev.* **1995**, *95*, 735.
- Li, X. Z.; Li, F. B.; *Environ. Sci. Technol.* **2001**, *35*, 2381.
- Zhou, G.; Deng, J.; *Mater. Sci. Semicond. Process.* **2007**, *10*, 90.
- Zheng, Y.; Zheng, L.; Zhan, Y.; Lin, X.; Zheng, Q.; Wei, K.; *Inorg. Chem.* **2007**, *46*, 6980.
- Zhang, Y.; Mu, J.; *J. Colloid Interface Sci.* **2007**, *309*, 478.
- Tan, T.; Li, Y.; Liu, Y.; Wang, B.; Song, X.; Li, E.; Wang, H.; Yan, H.; *Mater. Chem. Phys.* **2008**, *111*, 305.
- Xu, J.; Chang, Y.; Zhang, Y.; Ma, S.; Qu, Y.; Xu, C.; *Appl. Surf. Sci.* **2008**, *255*, 1996.
- Song, C.; Lin, Y.; Wang, D.; Hu, Z.; *Mater. Lett.* **2010**, *64*, 1595.
- Xie, W.; Li, Y.; Sun, W.; Huang, J.; Xie, H.; Zhao, X.; *J. Photochem. Photobiol., A* **2010**, *216*, 149.
- Ren, C.; Yang, B.; Wu, M.; Xu, J.; Fu, Z.; Lv, Y.; Guo, T.; Zhao, Y.; Zhu, C.; *J. Hazard. Mater.* **2010**, *182*, 123.
- Xie, J.; Wu, Q.; *Mater. Lett.* **2010**, *64*, 389.
- Gao, S.; Jia, X.; Yang, S.; Li, Z.; Jiang, K.; *J. Solid State Chem.* **2011**, *184*, 764.
- Lu, W.; Liu, G.; Gao, Sh.; Xing, Sh.; Wang, J.; *Nanotechnology* **2008**, *19*, 445711.
- Krishnan, D.; Pradeep, T.; *J. Cryst. Growth* **2009**, *311*, 3889.

37. Lin, D.; Wu, H.; Zhang, R.; Pan, W.; *Chem. Mater.* **2009**, *21*, 3479.
38. Sedlak, A.; Janusz, W.; *Physicochem. Probl. Miner. Process.* **2008**, *42*, 57.
39. Tahiri, H.; Ichou, Y. A.; Herrmann, J.-M.; *J. Photochem. Photobiol., A* **1998**, *114*, 219.
40. Arabatzis, I. M.; Stergiopoulos, T.; Andreeva, D.; Kitova, S.; Neophytides, S. G.; Falaras, P.; *J. Catal.* **2003**, *220*, 127.
41. Akpan, U. G.; Hameed, B. H.; *J. Hazard. Mater.* **2009**, *170*, 520.
42. Wang, J.; Xie, Y.; Zhang, Z.; Li, J.; Chen, X.; Zhang, L.; Xu, R.; Zhang, X.; *Sol. Energy Mater. Sol. Cells* **2009**, *93*, 355.
43. Hasnat, M. A.; Uddin, M. M.; Samed, A. J. F.; Alama, S. S.; Hossain S.; *J. Hazard. Mater.* **2007**, *147*, 471.

*Submitted: January 7, 2013*

*Published online: July 12, 2013*